Available online at www.sciencedirect.com

ScienceDirect

Ceramics International 37 (2011) 3299–3305

CERAMICS INTERNATIONAL

www.elsevier.com/locate/ceramint

# Estimation of mass transfer parameters during dehydroxylation in a large ceramic body by inverse methods

Ján Ondruška [a], Anton Trník [a,b,*], Igor Medved [a,b]

[a] Department of Physics, Constantine the Philosopher University, 949 74 Nitra, Slovakia
[b] Department of Materials Engineering and Chemistry, Czech Technical University, 166 29 Prague, Czech Republic

Received 16 May 2011; accepted 24 May 2011
Available online 30 May 2011

## Abstract

An inverse problem of the parameter estimation for the water transport during dehydroxylation in a large cylindrical ceramic body is solved. The transport is described by a standard type of non-stationary diffusion equation with a volumetric generation. The inverse problem is solved by the Levenberg–Marquardt method, with the estimated parameters being the water transfer diffusivity and water generation per unit volume. Their temperature dependencies are obtained within the dehydroxylation regime for 450 °C, 500 °C, 550 °C, and 600 °C, using experimental data from isothermal heating measurements. The activation energy of the diffusion process is estimated from the temperature dependence of the diffusivity, yielding 72.9 kJ $\text{mol}^{-1}$.

*Keywords:* C. Diffusion; C. Thermal properties; D. Porcelain

## 1. Introduction

Dehydroxylation is an endothermic reaction that occurs in kaolin based ceramics. This reaction is connected with the liberation of chemically bonded water from kaolinite crystals and the change of kaolinite to metakaolinite. It is generally accepted that a dehydroxylation begins at the temperature ~450 °C. However, some experimental measurements showed that the beginning of dehydroxylation could be shifted to the temperature ~420 °C [1]. It was also concluded that the more perfect the structure, the higher the temperature of dehydroxylation [2].

The chemical equation of dehydroxylation may be written as

$$8\text{OH}^- \rightarrow 4\text{H}_2\text{O(g)} + 4\text{O}^{2-}$$

considering that in a unit cell of kaolinite there are eight OH groups undergoing the above change [3]. Due to the liberation of water, kaolinite loses about 14% of its mass during dehydroxylation. As a result, the specific mass of kaolinite crystals decreases from 2.64 g $\text{cm}^{-3}$ to 2.51 g $\text{cm}^{-3}$, while its porosity increases from ~45% to ~50% [4].

Dehydroxylation occurs on a phase boundary, and its mechanism includes the transport of $\text{OH}^-$ groups to the phase boundary, the reaction of the groups on the boundary, and the transport of molecules $H_2O$ to the edge of the crystal. The rate of dehydroxylation is determined by the slowest process, which is the diffusion of the molecules $H_2O$ between layers of the kaolinite structure [2]. Thus, dehydroxylation is controlled by water diffusion. The activation energy of dehydroxylation for the degree of the conversion $0 < \alpha < 0.65$ is 140–190 kJ $\text{mol}^{-1}$ in dependence on the size and defects of kaolinite crystals; in smaller crystals the activation energy can be as low as 100 kJ $\text{mol}^{-1}$ [2,5,6].

In this paper we study dehydroxylation in a large ceramic body of cylindrical shape and show that the water diffusion can be described with good precision by a standard non-stationary diffusion equation with a volumetric generation term. Using isothermal experimental data on the rate of conversion of kaolinite into metakaolinite in the temperature range 450–600 °C where dehydroxylation takes place, we apply the Levenberg–Marquardt inverse method [7,8] to estimate the associated mass transfer diffusivity and the generation term in dependence on the temperature. In addition, we use these

---

* Corresponding author at: Department of Physics, Constantine the Philosopher University, 949 74 Nitra, Slovakia.
*E-mail addresses:* atrnik@ukf.sk, anton.trnik@fsv.cvut.cz (A. Trník).

0272-8842/$36.00 © 2011 Elsevier Ltd and Techna Group S.r.l. All rights reserved.
doi:10.1016/j.ceramint.2011.05.126

results to estimate the activation energy of the diffusion process.

## 2. Theoretical

We shall assume that the diffusion of water vapor through the samples during dehydroxylation can be described by the standard mass diffusion equation [9]

$$\frac{\partial \rho_w(r,t)}{\partial t} = \nabla \cdot [D \nabla \rho_w(r,t)] + g, \tag{1}$$

where $\rho_w$ and $D$ is the volume density and mass transfer diffusivity, respectively, of water vapor in a ceramic sample and $g$ is the volumetric generation of water vapor per unit volume of the sample. In isothermal heating the diffusivity $D$ and the generation term $g$ attain fixed values at a given temperature $T$. In order to estimate the parameters $D$ and $g$ as functions of $T$, we consider the rate of conversion of kaolinite into metakaolinite. Namely, we define the conversion coefficient as

$$\alpha(r,t) = \frac{\rho_p(r,t) - \rho_2}{\rho_1 - \rho_2}, \tag{2}$$

where $\rho_1$ and $\rho_2$ are the sample densities before and after dehydroxylation, respectively, and $\rho_p$ is the sample density after partial dehydroxylation. Note that $\alpha$ quantitatively determines the portion of the sample in which the dehydroxylation process has already taken place. At any time the ceramic body mass after partial dehydroxylation satisfies $m_p = m_w + m_m$, where $m_w$ is the time varying water vapor mass and $m_m$ = const is the body matrix mass. Since the body volume remains practically constant during dehydroxylation (the volume change is about 0.2%, see Fig. 1), we have $\rho_p = \rho_w + \rho_m$ with $\rho_m \approx$ const. Therefore, assuming that $\alpha$ is isotropic in the radial and axial directions, Eqs. (1) and (2) yield:

$$\frac{\partial \alpha(r,t)}{\partial t} = D \frac{1}{r} \frac{\partial}{\partial r}\left( r \frac{\partial \alpha(r,t)}{\partial r} \right) + \frac{g}{\rho_1 - \rho_2}, \tag{3}$$

where $r$ is the radial distance. Using experimentally obtained values of $\alpha$ in dependence on $r$ and $t$ during an isothermal heating, we shall use inverse methods to estimate the values of the mass transfer parameters $D$ and $g$.

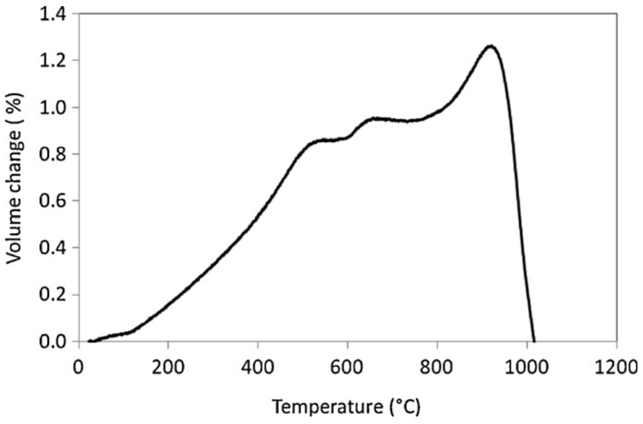

Fig. 1. The temperature dependence of the volume change.

### 2.1. Numerical estimation of mass transfer parameters

An inverse problem of estimating various kinetic parameters is opposed in formulation to a direct problem. In our case the direct problem is specified by solving Eq. (3) for $\alpha(r, t)$, provided an initial condition and boundary conditions are given and the parameters $D$ and $g$ are known functions of the temperature. This is a well-posed type of mathematical problem, for its solution satisfies the requirements of existence, uniqueness, and stability with respect to the input data [10]. On the other hand, the inverse problem consists in estimating $D$ and $g$ using Eq. (3) and an initial condition and boundary conditions, provided we know values of $\alpha(r, t)$ at several positions $r_k$ and times $t_l$ from measurements. Even though this is not a well-posed type of mathematical problem (in the above sense), it can be reformulated as such (for example, as a minimization problem [10]), and hence conveniently applied to parameter estimation (see [11–14], for example).

### 2.2. Formulation of the direct problem

The direct problem is given by Eq. (3) supplemented by an initial condition and boundary conditions. For the isothermal heating corresponding to a given temperature $T$, the initial condition reads

$$\alpha(r, t_{\mathrm{in}}) = \alpha_{\mathrm{in}}(r), \quad 0 \le r \le r_0, \tag{4}$$

where $\alpha_{\mathrm{in}}(r)$ is radial distribution of the conversion coefficient at an initial time $t_{\mathrm{in}}$ and $r_0$ is a maximal radial position for which Eq. (3) is solved. The boundary conditions read

$$\alpha(r_0, t) = \alpha_{\mathrm{bd}}(t), \qquad \frac{\partial \alpha(0,t)}{\partial r} = 0, \quad t_{\mathrm{in}} \le t \le t_{\mathrm{fin}}, \tag{5}$$

where $\alpha_{\mathrm{bd}}(t)$ is the time dependence of the conversion coefficient at $r_0$ and $t_{\mathrm{fin}}$ is a final time. The second boundary condition expresses the radial symmetry of the mass diffusion. As soon as values of $D$ and $g$ are known, Eqs. (3)–(5) can be solved, yielding a unique solution $\alpha(r, t)$ for $0 \le r \le r_0$ and $t_{\mathrm{in}} \le t \le t_{\mathrm{fin}}$. If the dependence of $\alpha$ on $D$ and $g$ will be of relevance, we shall write $\alpha_{D,g}(r, t)$ to stress this fact.

### 2.3. The inverse problem and its solution

In the inverse problem it is the parameters $D$ and $g$ that are to be determined, using experimental data on the radial and time dependencies of the conversion coefficient $\alpha$ measured during isothermal heating. Thus, given an isothermal heating temperature $T$, one experimentally obtains the values $\alpha_{kl}^{\mathrm{exp}}$ of the conversion coefficient at radial positions $0 \le r_k \le r_0$ ($k = 1, \ldots, n$) and times $t_{\mathrm{in}} \le t_l \le t_{\mathrm{fin}}$ ($l = 1, \ldots, m$). The inverse problem is reformulated as a minimization of the weighted least-square norm

$$S(\mathbf{p}) = [\boldsymbol{\alpha}^{\mathrm{exp}} - \boldsymbol{\alpha}^{\mathrm{est}}(\mathbf{p})]^{\mathrm{T}} \mathbf{W} [\boldsymbol{\alpha}^{\mathrm{exp}} - \boldsymbol{\alpha}^{\mathrm{est}}(\mathbf{p})], \tag{6}$$

where $\mathbf{p} = (D, g)$ is the vector of the estimated parameters, $\boldsymbol{\alpha}^{\mathrm{exp}} = (\alpha_{11}^{\mathrm{exp}}, \ldots, \alpha_{1m}^{\mathrm{exp}}, \alpha_{21}^{\mathrm{exp}}, \ldots, \alpha_{2m}^{\mathrm{exp}}, \ldots, \alpha_{n1}^{\mathrm{exp}}, \ldots, \alpha_{nm}^{\mathrm{exp}})$ is the vector of the measured values of the conversion coefficient,

$\boldsymbol{\alpha}^{\text{est}}(\mathbf{p}) = (\alpha_{D,g}(r_1, t_1), \ldots, \alpha_{D,g}(r_1, t_m), \alpha_{D,g}(r_2, t_1), \ldots, \alpha_{D,g}(r_2, t_m), \ldots, \alpha_{D,g}(r_n, t_1), \ldots, \alpha_{D,g}(r_n, t_m))$ is the vector of estimated values of the conversion coefficient at $r_k$ and $t_l$ as obtained from the solution of the direct problem with values $D$ and $g$, and $\mathbf{W}$ is a diagonal matrix with diagonal elements equal to the inverse $1/\sigma_{kl}^2$ of the variances of the measurements (the superscript T denotes the transposed matrix).

We solve the inverse problem by using the Levenberg–Marquardt method [7,8]. It is based on an iterative procedure in which the parameter vector $\mathbf{p}_{i+1}$ in the $(i + 1)$th step is related to the parameter vector $\mathbf{p}_i$ in the preceding step as $\mathbf{p}_{i+1} = \mathbf{p}_i + \Delta\mathbf{p}_i$, where

$$\Delta\mathbf{p}_i = (\mathbf{J}_i^{\mathrm{T}}\mathbf{W}\mathbf{J}_i + \mu_i\mathbf{I})^{-1}\mathbf{J}_i^{\mathrm{T}}\mathbf{W}[\boldsymbol{\alpha}^{\exp} - \boldsymbol{\alpha}^{\text{est}}(\mathbf{p}_i)]. \tag{7}$$

The sensitivity matrix $\mathbf{J}_i = \partial\boldsymbol{\alpha}^{\text{est}}(\mathbf{p}_i)/\partial\mathbf{p}_i$ is the $nm \times 2$ matrix whose two columns contain the elements $\partial a_{D_i,g_i}(r_k, t_l)/\partial D_i$ and $\partial a_{D_i,g_i}(r_k, t_l)/\partial g_i$, respectively, the number $\mu_i$ is the damping parameter, and $\mathbf{I}$ is the $2 \times 2$ unit matrix. The correction (6) is a combination of the Gauss–Newton method (obtained for $\mu_i \to 0$) that quickly converges and requires a good initial estimate of the parameters and of the steepest descent method (obtained for $\mu_i \to \infty$) that converges slowly but does not require a good initial estimate [10]. Therefore, at the beginning of the iteration procedure $\mu_i$ is usually taken large and then it is gradually decreased. Moreover, if instabilities are generated during the iteration procedure, $\mu_i$ should be increased, making the Levenberg–Marquardt method rather stable. The stopping criteria for the method are usually expressed as [10]

$$\sqrt{\frac{S(\mathbf{p}_{i+1})}{N}} \le \varepsilon_1, \quad \frac{\|\mathbf{p}_{i+1} - \mathbf{p}_i\|}{\|\mathbf{p}_{i+1}\|} \le \varepsilon_2,$$
$$\frac{|S(\mathbf{p}_{i+1}) - S(\mathbf{p}_i)|}{S(\mathbf{p}_{i+1})} \le \varepsilon_3,$$

where $N = nm$ is the total number of measured data, $\varepsilon_1$, $\varepsilon_2$, and $\varepsilon_3$ are prefixed positive tolerances, and $\|\cdot\|$ is a vector norm. As soon as each of these criteria is satisfied, the iterative procedure is stopped.

### 2.4. The solution algorithm

The solution algorithm for the Levenberg–Marquardt method may slightly vary, depending on the specific problem. Here we shall employ the version that consists of the following steps.

1. Using the estimated values $D_i$ and $g_i$ from the $i$th step, we numerically solve the direct problem, Eqs. (3)–(5), yielding $\alpha_{D_i,g_i}(r, t)$ for $0 \le r \le r_0$ and $t_{\text{in}} \le t \le t_{\text{fin}}$. The vector $\boldsymbol{\alpha}^{\text{est}}(\mathbf{p}_i)$ is then obtained by plugging the positions $r_k$ and times $t_l$ into the solution $\alpha_{D_i,g_i}(r, t)$. The norm $S(\mathbf{p}_i)$ is evaluated from Eq. (6).
2. We numerically solve the direct problem two more times, once for the parameters $D_i + \Delta D_i$ and $g_i$ and once for the parameters $D_i$ and $g_i + \Delta g_i$. From these two solutions we get the values $\alpha_{D_i+\Delta D_i,g_i}(r_k, t_l)$ and $\alpha_{D_i,g_i+\Delta g_i}(r_k, t_l)$ for all $r_k$ and $t_l$.
3. The sensitivity coefficients matrix $\mathbf{J}_i$ is then computed, using the approximations
$$\frac{\partial\alpha_{D_i,g_i}(r_k, t_l)}{\partial D_i} \approx \frac{\alpha_{D_i+\Delta D_i,g_i}(r_k, t_l) - \alpha_{D_i,g_i}(r_k, t_l)}{\Delta D_i} \tag{9}$$
and
$$\frac{\partial\alpha_{D_i,g_i}(r_k, t_l)}{\partial g_i} \approx \frac{\alpha_{D_i,g_i+\Delta g_i}(r_k, t_l) - \alpha_{D_i,g_i}(r_k, t_l)}{g_i}. \tag{10}$$
4. The estimated values $D_{i+1}$ and $g_{i+1}$ in the $(i + 1)$th step are computed from the relation $\mathbf{p}_{i+1} = \mathbf{p}_i + \Delta\mathbf{p}_i$ with $\Delta\mathbf{p}_i$ given by Eq. (7).
5. The direct problem is numerically solved, yielding the vector $\boldsymbol{\alpha}^{\text{est}}(\mathbf{p}_{i+1})$ and the norm $S(\mathbf{p}_{i+1})$.
6. If $S(\mathbf{p}_{i+1}) \ge S(\mathbf{p}_i)$, we set $\mu_{i+1} = 10\mu_i$, unless $\mu_i > 10^{20}$. Otherwise we set $\mu_{i+1} = 0.1\mu_i$.
7. If none of the stopping criteria (8) is satisfied, the calculations are repeated.

## 3. Experimental

Samples were prepared from wet plastic ceramic mass by the electro-porcelain plant PPC Čab, Slovakia, a member of the international PPC Insulators group. The initial composition of ceramic material consists of 48 wt.% of kaolin and clay,

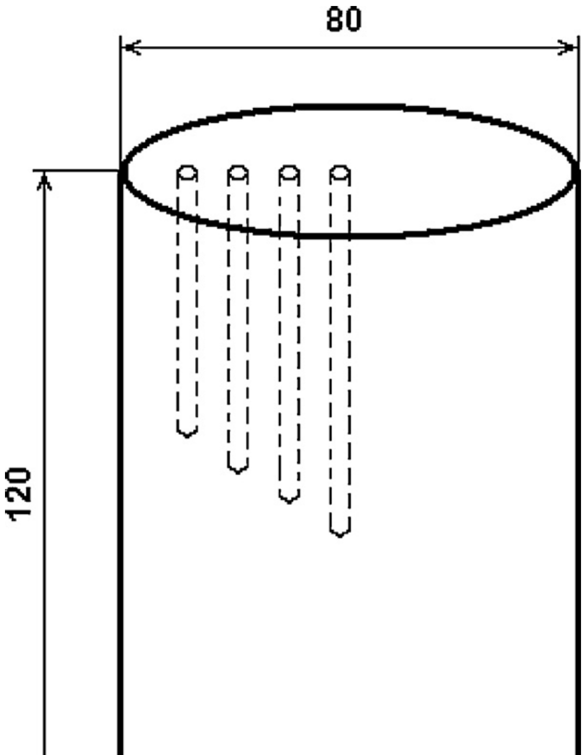

Fig. 2. Cylindrical sample with holes for thermocouples. The dimensions are in mm.

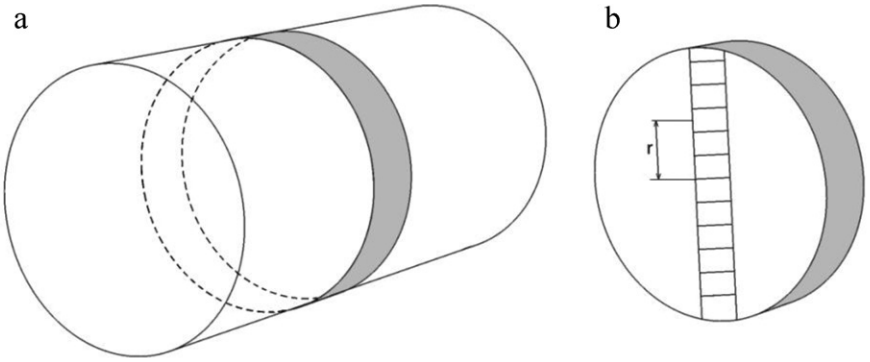

Fig. 3. (a) Cylindrical blank and (b) a 10 mm thin disc with a small samples 10 mm × 10 mm × 5 mm.

30 wt.% of alumina and 22 wt.% of feldspar. The samples have a cylindrical shape of diameter 80 mm and length 120 mm. Four holes (∅2 mm) in which thermocouples Pt–PtRh10 were placed were bored in the samples as shown in Fig. 2.

First, the samples were dried in the furnace in the isothermal regime at 150 °C for 8 h. The temperature 150 °C was reached by linear heating with the heating rate 0.5 °C $\mathrm{min}^{-1}$. Then the samples were cooled to the room temperature.

The measurements were performed in the temperature interval where the dehydroxylation takes place. Namely, we used the isothermal temperatures $T_{\mathrm{iso}} = 450$ °C, 500 °C, 550 °C, and 600 °C. The temperature $T_{\mathrm{iso}}$ was kept constant for a period of time 0, 1, 2, 3, 4, 5, 6, 7, 8, 9 and 10 h. A disc of 10 mm thick was cut from the middle of the cooled sample (see Fig. 3a). A prism 10 mm × 10 mm × 80 mm was cut from the disc and the prism was divided into small blocks 10 mm × 10 mm × 5 mm as shown in Fig. 3b. The mass $m$ of the small blocks was measured on laboratory balance with sensitivity $2 \times 10^{-6}$ g. Then we put small blocks to the furnace for isothermal heating at 1000 °C for 8 h (at 1000 °C we may safely assume that dehydroxylation ceased to take place). The mass of the cooled small blocks was measured again and the mass difference $\Delta m$ was obtained for each small block.

We focused on the conversion coefficient $\alpha$ which depends on the concentration of the constituent water in kaolinite crystal [15]. For our purpose we define conversion coefficient $\alpha$ as

$$\alpha = \frac{\Delta m_0/m_0 - \Delta m/m}{\Delta m_0/m_0}, \tag{11}$$

where $m_0$ is the mass of a raw reference sample and $\Delta m_0$ is difference between the masses of the raw reference sample before and after full dehydroxylation [16].

## 4. Results and discussion

### 4.1. Implementation of the inverse analysis

The points $r_k$ are chosen to coincide with the radial positions at which the conversion coefficient $\alpha$ was measured, i.e., $r_k = 0.25$ cm, 0.75 cm, 1.25 cm, …, 3.75 cm, and $r_0$ is identified with the largest of these positions, $r_0 = 3.75$ cm. Hence, the total number of the radial positions $r_k$ is $n = 8$.

The initial time $t_{\mathrm{in}}$ is chosen for each of the isothermal heating temperatures $T_{\mathrm{iso}}$ separately in such a way that a maximal difference, $\Delta T_{\mathrm{max}}$, of the temperature recorded in a cylindrical sample (at all radial positions $0 \leq r \leq r_0$ and all times $t_{\mathrm{in}} \leq t \leq t_{\mathrm{fin}}$) with respect to $T_{\mathrm{iso}}$ is at most 2 °C. This guarantees that $D$ and $g$ can be reliably attributed to a given temperature $T_{\mathrm{iso}}$. The specific choices of the initial time for a given $T_{\mathrm{iso}}$ are listed in Table 1. The final time $t_{\mathrm{fin}}$ is fixed and set equal to 10 h (the time when the isothermal heating measurements are ended). The times $t_l$ at which the values $\alpha_{kl}^{\mathrm{exp}}$ are measured are 1 h separated, i.e., $t_l = t_{\mathrm{in}}, t_{\mathrm{in}} + 1, \ldots, t_{\mathrm{fin}}$. The number of these times $m$ depends on the choice of $t_{\mathrm{in}}$ and can be obtained from Table 1.

We applied the Levenberg–Marquardt iterative procedure, using Eq. (7). For simplicity, we assumed that measurement errors were independent and identically distributed so that the variances of the measurements were constant, $\sigma_{kl}^2 = \mathrm{const} = \sigma^2$ Then the multiplication by the matrix $\mathbf{W}$ in Eq. (7) reduces just to the rescaling of the damping parameter (from $\mu_i$ to $\sigma^2\mu_i$), which can be included in a choice of the value of $\mu_i$ and, hence, need not be specified in the following. The starting value of the damping parameter was taken as $\mu_0 = 0.001$, while the staring values of the mass transfer diffusivity and volumetric generation were $D_0 = 5 \times 10^{-5}\ \mathrm{m}^2\ \mathrm{s}^{-1}$ and $g_0 = 100\ \mathrm{mg\ m}^{-3}\ \mathrm{s}^{-1}$, respectively. Moreover, we used $\Delta D_i = 0.1 D_i$, $\Delta g_i = 0.1 g_i$, $\varepsilon_2 = 0.001$, and $\varepsilon_3 = 2 \times 10^{-5}$. The value of $\varepsilon_1$ was tailored to a given temperature $T_{\mathrm{iso}}$ and is listed in Table 1.

### 4.2. Diffusivity and volumetric generation

The estimated values of the mass transfer diffusivity $D$ and volumetric generation $g$ as resulting from the inverse analysis

Table 1
The set of initial parameters for the inverse analysis.

| | $T_{\mathrm{iso}}$ (°C) | | | |
|---|---|---|---|---|
| | 450 | 500 | 550 | 600 |
| $t_{\mathrm{in}}$ (h) | 3 | 2 | 6 | 7 |
| $\Delta T_{\mathrm{max}}$ (°C) | 0.8 | 1.6 | 1.3 | 0.8 |
| $m$ | 8 | 9 | 5 | 4 |
| $\varepsilon_1$ | 0.005 | 0.017 | 0.045 | 0.009 |

Table 2
The estimated values of the transport parameters.

| | $T_{\mathrm{iso}}$ (°C) | | | |
|---|---|---|---|---|
| | 450 | 500 | 550 | 600 |
| $D$ ($\times 10^{-6}$ m$^2$ s$^{-1}$) | 3.61 | 5.73 | 16.8 | 25.7 |
| $g$ ($\times 10^{-4}$ kg m$^{-3}$ s$^{-1}$) | 0.52 | 0.88 | 5.45 | 1.95 |

are given in Table 2. In the calculations we used the density values $\rho_1 = 1868$ kg m$^{-3}$ and $\rho_2 = 1820$ kg m$^{-3}$.

The temperature dependence of the diffusivity is expected to follow the Arrhenius-type of law [17,18],

$$D = D_0 e^{-E_a/RT}, \tag{12}$$

where $D_0$ is the diffusivity at infinite temperature, $E_a$ is the activation energy corresponding to the process of vapor diffusion, and $R$ is the gas constant. In that case the plot of ln $D$ vs. 1/$RT$ should be a straight line with a negative slope coinciding with $E_a$. This plot, as obtained from the data of Table 2, is shown in Fig. 4. We observe that, in fact, the four plotted points follow approximately a straight line. Applying a best-fit analysis, we get that the slope of this line yields the activation energy $E_a = 72.9$ kJ mol$^{-1}$. This is in good agreement with values obtained for the studied ceramic material independently by different methods (used specifically for the evaluation of $E_a$) [19].

The temperature dependence of the volumetric generation $g$ should reflect upon the dehydroxylation process that takes place within the considered temperature range 450–600 °C. As the effect of dehydroxylation becomes stronger, values of $g$ should grow, whereas when dehydroxylation is coming to an end, values of $g$ should decrease. Hence, a peak is expected to occur in a $g$ vs. $T$ plot. Our values of $g$ in dependence on $T$ from Table 2 follow exactly this type of behavior as is shown in Fig. 5.

### 4.3. Conversion parameter

Figs. 6–9 show experimental and theoretical results of the dependence of the conversion coefficient $\alpha$ on the temperature $T_{\mathrm{iso}}$, radial position $r$ and time $t_l$. It is clear that dehydroxylation starts on the surface of the sample ($r = 4$ cm) and spreads into its center.

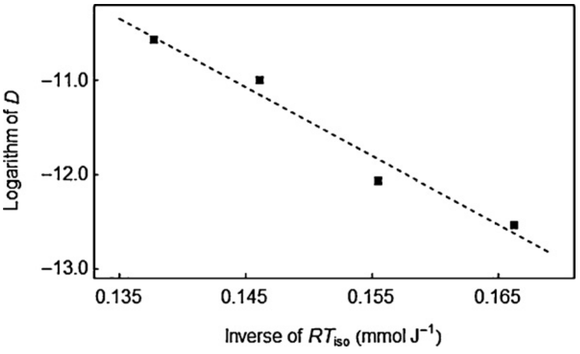

Fig. 4. The logarithm of mass diffusivity in dependence on 1/$RT_{\mathrm{iso}}$.

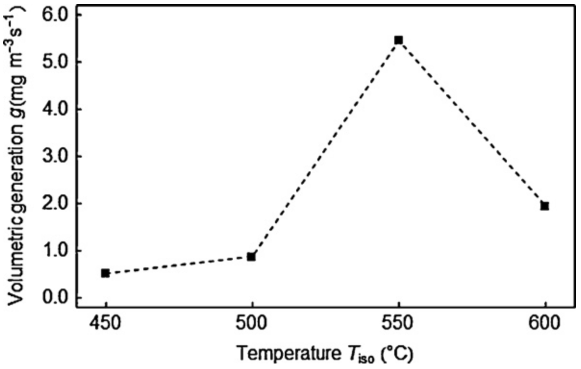

Fig. 5. The temperature dependence of the volumetric generation.

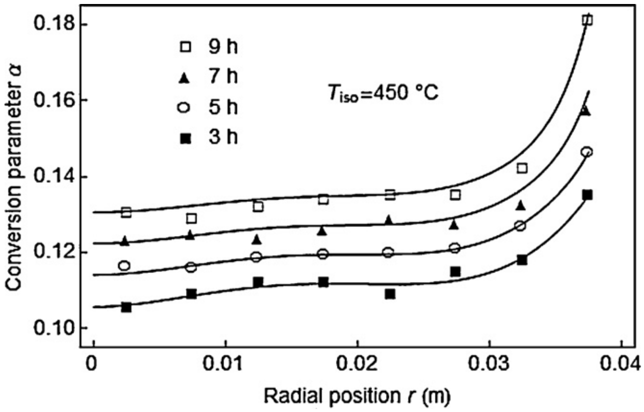

Fig. 6. The radial position dependence of the conversion parameter $\alpha$ for the isothermal temperature 450 °C. Experimental data are represented by points, theoretical dependences are shown by lines.

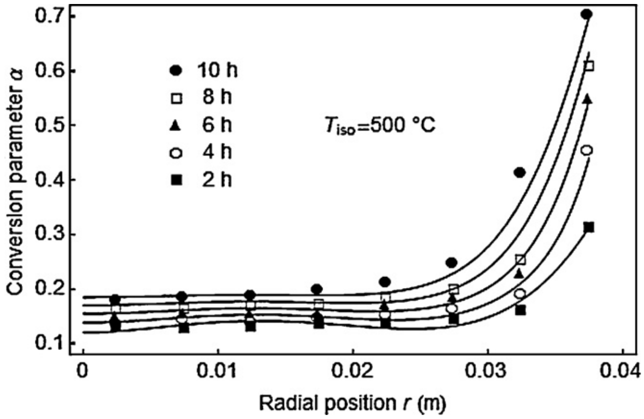

Fig. 7. The radial position dependence of the conversion parameter $\alpha$ for the isothermal temperature 500 °C. Experimental data are represented by points, theoretical dependences are shown by lines.

The results depicted in Fig. 6 show that at the temperature 450 °C, the conversion coefficient does not vary significantly with the radial position, because the dehydroxylation process runs slowly at that temperature. Also numerical results are in very good agreement with experimental data, the largest relative error being ∼6%. The differences between different times $t_l$ may be caused by the liberation of water molecules bounded on the surface of the kaolinite crystals [20].

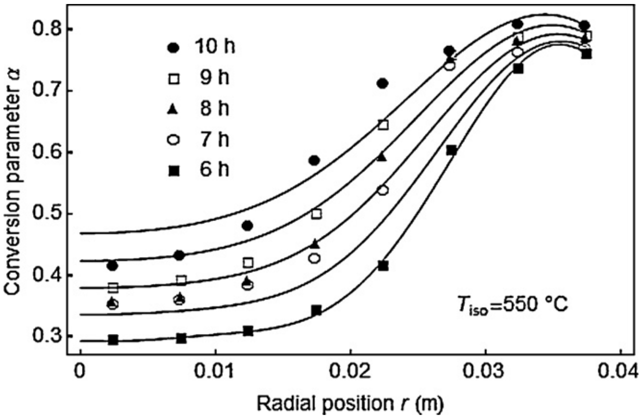

Fig. 8. The radial position dependence of the conversion parameter α for the isothermal temperature 550 °C. Experimental data are represented by points, theoretical dependences are shown by lines.

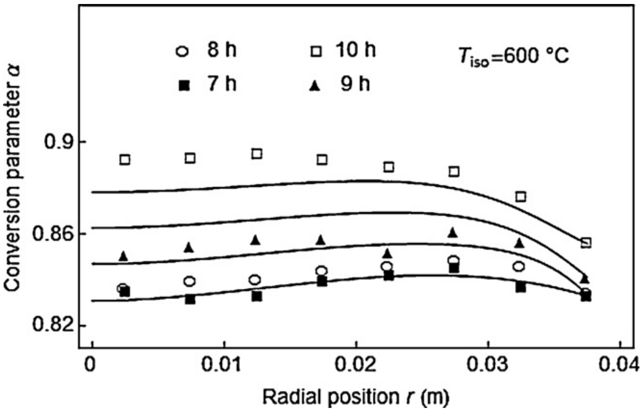

Fig. 9. The radial position dependence of the conversion parameter α for the isothermal temperature 600 °C. Experimental data are represented by points, theoretical dependences are shown by lines.

In Fig. 7 the radial position dependence of α at 500 °C is rather profound. It shows that up to 60% of kaolinite has been transformed to metakaolinite near the surface (for radial positions 3–4 cm). Nevertheless, the relative errors between experimental and numerical results are still relatively small, up to ∼22%.

Figs. 8 and 9 show that an increasing amount of metakaolinite occurs as the isothermal temperature grows to 600 °C and that dehydroxylation takes place closer and closer to the center of the sample. For 550 °C up to 50% of kaolinite has been transformed in the center of the sample, while for 600 °C this is even ∼85%. This indicates that the dehydroxylation terminates at temperatures slightly above 600 °C. This time the relative errors of numerical results with respect to the experimental ones are smaller, up to ∼14% for 550 °C and only up to ∼2% for 600 °C. Although at temperatures where dehydroxylation is most intensive (around 550 °C) the simple model, Eq. (3), cannot describe the water diffusion process in all its complexity, the obtained numerical results are in rather good agreement with the experiments.

A surprising result was obtained for higher $T_{iso}$ and longer $t_l$ (see Fig. 9) where the conversion coefficient for large radial positions is lower than near the center [16]. This may be attributed to a systematic error due to the mass of the small blocks that contain physically bounded water. The decrease of the conversion coefficient in large radial positions could be also caused during cooling when the sample absorbs air humidity. Moreover, the decrease of α may be also a consequence of the production of the samples that were cut out from the wet plastic ceramic mass using an extruder, and so kaolinite crystals in large radial positions have different orientations than in the center [21,22].

In numerical analysis this anomaly behavior of α for large r was taken into account by the choice of the initial conditions. Indeed, since the initial times $t_{in}$ for the temperatures 550 °C and 600 °C are 6 h and 7 h, respectively, the initial condition itself contains this behavior.

## 5. Conclusions

We have used an inverse analysis to estimate transport parameters for the diffusion of water vapor during the dehydroxylation process in a large ceramic body. The diffusion was described by a non-stationary diffusion equation with a volumetric generation. Hence, the estimated parameters were the water diffusivity D and water generation per unit volume g. The two parameters were assumed to be constant for a given temperature. Using experimental data on the rate α of conversion of kaolinite into metakaolinite from isothermal heating measurements at the temperatures 450 °C, 500 °C, 550 °C, and 600 °C (when dehydroxylation occurred in the samples), we applied the Levenberg–Marquardt iterative procedure to solve the inverse problem and estimate D and g in dependence on the temperature. Although the employed diffusion model is rather simple, we obtained numerical results in good agreement with the experimental ones. We also fitted the temperature dependence of D by the Arrhenius law and thus estimated the activation energy of the diffusion process to be 72.9 kJ $mol^{-1}$.

## Acknowledgements

This research was supported by the VEGA under Grant No. 1/0302/09 and by the Ministry of Education, Youth and Sports of the Czech Republic under the project No. MSM: 6840770031.

## References

[1] International Critical Tables of Numerical Data, Physics, Chemistry and Technology, 1st Electronic Edition, Washburn, E.W. ©1926–1930, Knovel, 2003.
[2] B. Čı́čel, I. Novák, I. Horváth, Mineralogy and Crystallochemistry of Clays, SAV, Bratislava, 1981.
[3] I. Štubňa, G. Varga, A. Trník, Investigation of kaolinite dehydroxylation is still interesting, Épı́tőanyag 58 (2006) 6–9.
[4] I. Štubňa, T. Kozı́k, Permeability of the electroceramics to gas and its dependence on the firing temperature, Ceram. Int. 23 (1997) 247–249.

[5] I. Horváth, Sedlec kaolinite dehydroxylation kinetics, in: Proc. 7th Conf. Clay Mineral. and Petrol., Karlovy Vary, (1976), pp. 121–127.

[6] I. Horváth, G. Kranz, Thermoanalytic study of the high-temperature dehydratation of kaolins with different degree of the order, Silikáty 24 (1980) 149–156.

[7] K. Levenberg, A method for the solution of certain nonlinear problems in least squares, Quart. Appl. Math. 2 (1944) 164–168.

[8] D.W. Marquardt, An algorithm for least squares estimation of nonlinear parameters, J. Soc. Ind. Appl. Math. 11 (1963) 431–441.

[9] P. Majumdar, Computational Methods for Heat and Mass Transfer, Taylor & Francis, New York, 2005.

[10] M.N. Özisik, H.R.B. Orlande, Inverse Heat Transfer: Fundamentals and Applications, Taylor & Francis, New York, 2000.

[11] L.B. Dantas, H.R.B. Orlande, R.M. Cotta, An inverse problem of parameter estimation for heat and mass transfer in capillary porous media, Int. J. Heat Mass Transfer 46 (2003) 1587–1598.

[12] W.M. Brasil, J. Su, A.P. Silva Freire, An inverse problem for the estimation of upstream velocity profiles in an incompressible turbulent boundary layer, Int. J. Heat Mass Transfer 47 (2004) 1267–1274.

[13] S. Rouquette, J. Guo, P. Le Masson, Estimation of the parameters of a Gaussian heat source by the Levenberg–Marquardt method: application to the electron beam welding, Int. J. Thermal Sci. 46 (2007) 128–138.

[14] N. Ukrainczyk, Thermal diffusivity estimation using numerical solution for 1D heat conduction, Int. J. Heat Mass Transfer 52 (2009) 5675–5681.

[15] W.M. Carty, U. Senapati, Porcelain—raw materials, processing, phase evolution, and mechanical behavior, J. Am. Ceram. Soc. 81 (1998) 3–20.

[16] J Ondruška, A. Trník, L. Vozár, Degree of conversion of dehydroxylation in a large electroceramic body, Int. J. Thermophys. 32 (2011) 729–735.

[17] J.W. Ross, R.J. Good, Adsorption and surface diffusion of normal-butane on spheron-6 (2700-degrees) carbon black, J. Phys. Chem. 60 (1956) 1167–1171.

[18] A.K. Galwey, M.E. Brown, Kinetic background to kinetic analysis and calorimetry, Handb. Thermal Anal. Calorim. 1 (1998) 147–217.

[19] J.N. Weber, R. Roy, Dehydroxylation of kaolinite, dickite and halloysite—heats of reaction and kinetics of dehydroxylation at $P_{H2O}$ = 15 psi, Am. Mineral. 50 (1965) 1038–1045.

[20] I Štubňa, L. Vozár, The influence of the sample size on low-temperature processes in green electroceramics, Ind. Ceram. 25 (2005) 110–112.

[21] I. Štubňa, A. Lintnerová, A. Trník, Mechanical properties and thermal expansion of clay ceramics measured on laboratory samples, Ind. Ceram. 29 (2009) 39–42.

[22] M. Kaluzná, L. Vozár, J. Gembarovič, I. Kaprálik, The effect of texture on the thermal-diffusivity of a ceramic material, Ceram. Silikáty 36 (1992) 15–19.